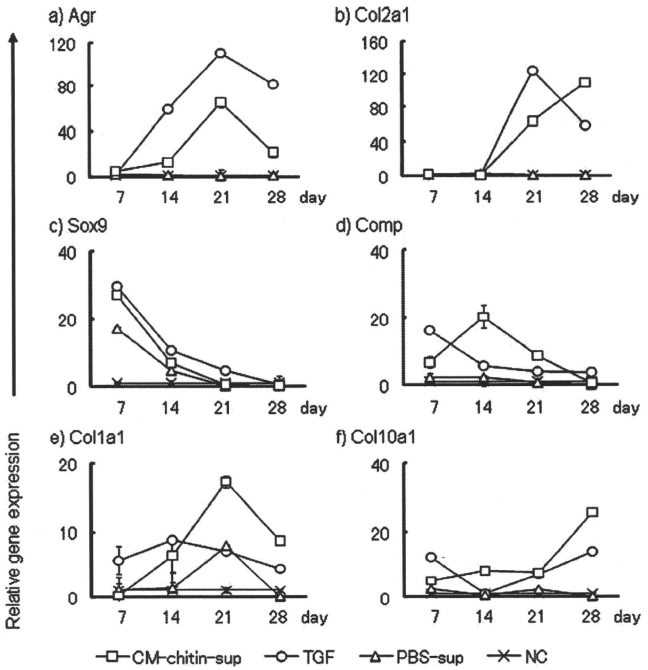


**FIGURE 3.** Quantitative mRNA expression of cartilage-related genes in micromass tissues. Micromass tissues were treated with TGF-β1 (10 ng/mL), PBS-conditioned medium (PBS-sup) or CM-chitin–conditioned medium (CM-chitin-sup) for 7, 14, 21, or 28 days, and their gene expression was compared with that of nontreated micromass tissue (NC). Data are expressed as the mean ± SE of three independent experiments. mRNA expression was normalized to that of GAPDH.

genesis in micromass culture, the mRNA expression of six chondrogenic markers in micromass tissues was quantified by Q-PCR. The mRNA expression of Agr and Col2a1 was significantly increased in the CM-chitin-sup treated samples on day 21, as well as in the TGF-β1–treated samples [Fig. 3(a,b)]. In the CM-chitin-sup treated micromass culture, the expression of Agr was found to be diminished on day 28, while the expression of Col2a1 was further increased on day 28 [Fig. 3(a,b)]. Sox9 and Comp mRNA were highly expressed on day 7 (Sox9) and 14 (Comp), but no expression was observed on day 28 [Fig. 3(c,d)]. Relatively high expression of Col1a1 and Col10a1 was also observed on days 21 and 28, respectively [Fig. 3(e)].

mRNA expression related to chondrogenesis was blocked by anti-TGF-β1 antibody (Fig. 4). The Agr, Co2a1, and Sox9 expression levels in the CM-chitin-sup and TGF-β1–treated micromass cultures were significantly decreased in the presence of the antibody.

### Histological analysis of micromass culture

To examine whether the growth factors secreted from PEC stimulated by CM-chitin induce chondrogenesis, the accumulation of chondrogenesis-related ECM in the micromass tissues was investigated by staining with Alcian blue, Toluidine blue, and anti-Collagen II antibody. The specific aggregation of micromass tissues was observed in the TGF-β1–treated micromass culture and CM-chitin-sup treated micromass culture [Fig. 5(a)]. However, neither the non-treated micromass culture nor the PBS-sup treated micromass culture formed 3D aggregates.

In the presence of TGF-β1 or CM-chitin-sup, the tissues showed a strong blue color under Alcian blue staining [Fig. 5(a,b)] and a magenta color under Toluidine blue staining [Fig. 5(c)], indicating the presence of sulfated glycosaminoglycan.[33] Immunohistological staining also showed the presence of collagen II in these micromass tissues [Fig. 5(d)]. The micromass tissues collected on day 7 or 14 were also subjected to staining, but no marked staining was observed

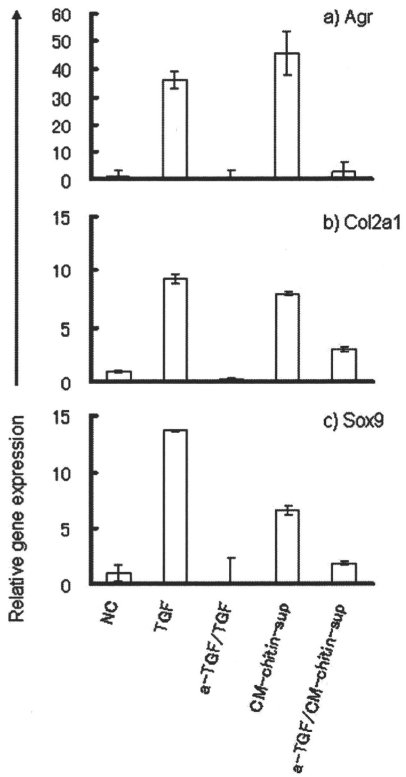


**FIGURE 4.** TGF-β1 blocking experiment using anti-TGF-β1 antibody. Micromass tissues were treated with TGF-β1 (TGF, 10 ng/mL), anti-TGF-β1 antibody + TGF-β1 (a-TGF/TGF, a-TGF = 10 μg/mL), CM-chitin–conditioned medium (CM-chitin-sup), or anti-TGF-β1 antibody + CM-chitin conditioned medium (a-TGF/CM-chitin-sup, a-TGF = 10 μg/mL), and their gene expression was compared with that of nontreated micromass tissues (NC). Micromass tissues were used for QPCR analysis of aggrecan (Agr), Collagen-2a1 (Col2a1), and Sox9 at the highest expression point of each gene (at days 21, 21, and 7, respectively). Data are expressed as the mean ± SE of three independent experiments. mRNA expression was normalized to that of GAPDH.

(data not shown). In contrast, the tissues treated with nothing or PBS-sup showed a weak blue color under Alcian blue staining and a blue color under Toluidine blue staining, indicating the absence of chondrogenesis-related ECM.

## DISCUSSION

We previously reported that CM-chitin induced the regeneration of hyaline cartilage in rabbits *in vivo*.[22] In contrast to conventional scaffold-based tissue-engineering methods using growth factors, no growth factor is required in our CM-chitin–based method, suggesting that CM-chitin has dual functions, as a scaffold and an inducer of cartilage-differentiation. We, therefore, investigated whether CM-chitin directly affects the cartilage differentiation of progenitor cells. The murine pluripotent cell line C3H10T1/2 was used in the present study. CM-chitin did not significantly alter the viability or proliferation of the cells [Fig. 1(a,b)], similarly to other biomaterials, such as polylactic acid,[34] polylactic acid–polyglycolic acid,[35] poly(DL-lactic-*co*-glycolic acid),[36] and silk.[7,37] Furthermore, CM-chitin did not influence the expression of growth factor or chondrogenic markers in C3H10T1/2 cells (Fig. 2). These results indicate that CM-chitin did not contribute directly to the differentiation of pluripotent cells into chondrocytes.

We recently found that CM-chitin stimulates immune cells to produce TGF-β1, a growth factor for cartilage regeneration.[23] However, it was unclear whether the stimulation of cells by CM-chitin leads to cartilage regeneration. We demonstrated here that the factors secreted from cells stimulated by CM-chitin induced the expression of chondrogenic markers. Micromass tissue of C3H10T1/2 cells, cultured in the presence of CM-chitin-sup, expressed mRNA of chondrogenic markers including aggrecan and type II collagen (Fig. 3).

Agrrecan (Agr), type II collagen (Col2a1), and Sox9 are *in vivo* and *in vitro* markers of chondrogenesis. Agr is an integral part of ECM components in cartilage,[38–41] and its expression is induced by several factors including TGF-β1, TGF-β3, BMP-2, and dexamethasone in micromass culture, pellet culture, or an appropriate 3D culture.[42–46] TGF-β1 is reported to promote the expression of Col2a1 and Sox9.[47] Sox9, a transcription factor, acts during chondrocyte differentiation and activates the transcription of Agr and Col2a1.[40,48,49] Type II collagen, which includes an α-1 chain encoded by Col2a1, is the most abundant and important component of the chondrogenesis-related ECM, and mutations in this gene are associated with achondrogenesis and chondrodysplasia.[50,51] It has also been shown in previous studies that the expression of Col2a1 was accompanied by an increase in Agr or glycosaminoglycan expression during chondrogenesis.[52–54] The time-courses of the expression of Sox9, Col2a1, and Agr in the present study [Fig. 3(a–c)] were coincident with the results of the above reports. In our results, the expression of Agr was decreased in both the TGF-β1–treated micromass culture and CM-chitin–treated micromass culture at day 28 [Fig. 3(a)]; whereas, Col2a1 expression was increased in the CM-chitin–treated micromass culture while its expression was decreased in the TGF-β1–treated micromass culture at day 28 [Fig. 3(b)]. Previous research of murine limb-bud-cell micromass culture reported that the high expression of Col2a1 decreases gradually and that the expression of collagen10, which is commonly observed in hypertrophic cartilage, is replaced by Col2a1 expression.[27] In our experiment, the Col2a1 and Col10a1 expression in TGF-β1–treated micromass culture seemed to correspond with above mentioned report [Fig. 3(b,f)]. On the other hand, the Col2a1 and Col10a1

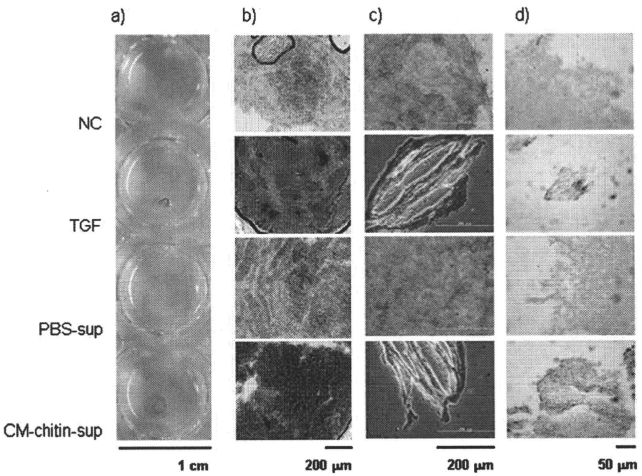


**FIGURE 5.** Histological evaluation of micromass tissues. (a) Alcian blue staining of tissues on day 21, observed at low magnification. (b) Alcian blue staining of tissues on day 21, observed at high magnification. (c) Toluidine blue staining of tissues on day 28. Tissues containing acidic glycosaminoglycan were stained a deep magenta color. (d) Immunohistological staining of tissues on day 28 with anti-collagen II antibody. Tissues containing collagen II were stained deep brown. In Figures (c and d), samples of TGF-β1 medium (TGF) and CM-chitin conditioned medium (CM-chitin-sup) were paraffinized, sectioned (12 μm), and deparaffinized before staining, while nontreated (NC) and PBS-conditioned medium (PBS-sup) treated tissues were not subjected to sectioning. [Color figure can be viewed in the online issue, which is available at www.interscience.wiley.com.]

expression in the CM-chitin treated micromass culture did not. The differences in Col2a1, Comp, and Col1a1 expression between the CM-chitin–treated and TGF-β1–treated micromass cultures [Fig. 3(b,d,e)] were probably due to another factor secreted from PEC, but this remains to be elucidated. We also showed here that blocking the TGF-β1 signal with anti-TGF-β1 antibody inhibited the expression of chondrogenic markers [Fig. 4(a–c)]. This indicated that TGF-β1 is one of the most important factors for chondrogenesis in micromass culture using CM-chitin-sup.

It has also been shown in previous studies that Comp, cartilage-oligomeric-protein, binds to collagen types I and II in the ECM and facilitates their structural stability.[55,56] Although Comp is synthesized by chondrocytes, osteoblasts, tenocytes, and ligament cells *in vivo*,[57,58] it is also synthesized by several mesenchymal cell–derived chondrocytes *in vitro*.[49,59,60] It was also reported that several types of TGF-β promote the expression of Comp in chondrogenic tissue from MSC.[61] Our result, which showed enhancement of Comp expression in micromass tissue due to treatment with TGF-β1 or CM-chitin-sup, is consistent with this report.

Histological evaluation showed the induction of glycosaminoglycan and type II collagen in CM-chitin-sup–treated micromass tissue (Fig. 5). Furthermore, a specific aggregation pattern was observed in the micromass tissue [Fig. 5(a)]. It has been reported that the treatment of micromass cultures of C3H10T1/2 cells with TGF-β1 resulted in the formation of a 3D spheroid culture exhibiting cartilage-like histology.[28,30] The aggregation pattern of the CM-chitin-sup–treated micromass tissue closely resembled that of the TGF-β1–treated micromass tissue [Fig. 5(a)], suggesting that the factors secreted by cells stimulated by CM-chitin–induced chondrogenesis in micromass culture.

Our results obtained in the present and previous studies suggested that the stimulation of CM-chitin induces the secretion of TGF-β1 from immune cells and results in the promotion of chondrogenesis in micromass culture. This shows that CM-chitin plays dual roles in cartilage regeneration as a scaffold and growth factor inducer. Recently, Yasuda et al. developed a novel method for inducing spontaneous *in vivo* cartilage regeneration by implanting a double-network hydrogel material into osteochondral defects of the femoral joint.[62] They observed spontaneous *in vitro* and *in vivo* chondrogenesis using a functional polymeric compound. Here, we also observed spontaneous *in vitro* chondrogenesis with a CM-chitin polymer without using any additional growth factors. Although the mechanism of the induction of TGF-β1 production in immune cells treated with CM-chitin has not been clarified, the CM-chitin–based cartilage regeneration method is a good candidate for tissue engineering as it does not require growth factors.

## References

1. Shapiro F, Koide S, Glimcher MJ. Cell origin and differentiation in the repair of full-thickness defects of articular cartilage. J Bone Joint Surg Am 1993;75:532–553.

2. Oka M. Biomechanics and repair of articular cartilage. J Orthop Sci 2001;6:448–456.
3. Ochi M, Adachi N, Nobuto H, Yanada S, Ito Y, Agung M. Articular cartilage repair using tissue engineering technique—Novel approach with minimally invasive procedure. Artif Organs 2004; 28:28–32.
4. Tuan RS, Boland G, Tuli R. Adult mesenchymal stem cells and cell-based tissue engineering. Arthritis Res Ther 2003;5:32–45.
5. Erggelet C, Steinwachs MR, Reichelt A. The operative treatment of full thickness cartilage defects in the knee joint with autologous chondrocyte transplantation. Saudi Med J 2000;21:715–721.
6. Kim UJ, Park J, Kim HJ, Wada M, Kaplan DL. Three-dimensional aqueous-derived biomaterial scaffolds from silk fibroin. Biomaterials 2005;26:2775–2785.
7. Wang Y, Kim UJ, Blasioli DJ, Kim HJ, Kaplan DL. In vitro cartilage tissue engineering with 3D porous aqueous-derived silk scaffolds and mesenchymal stem cells. Biomaterials 2005;26:7082–7094.
8. Lu L, Zhu X, Valenzuela RG, Currier BL, Yaszemski MJ. Biodegradable polymer scaffolds for cartilage tissue engineering. Clin Orthop Relat Res 2001;391:S251–S270.
9. Reinholz GG, Lu L, Saris DB, Yaszemski MJ, O'Driscoll SW. Animal models for cartilage reconstruction. Biomaterials 2004;25: 1511–1521.
10. Kimura T, Yasui N, Ohsawa S, Ono K. Chondrocytes embedded in collagen gels maintain cartilage phenotype during long-term cultures. Clin Orthop Relat Res 1984;186:231–239.
11. Chiroff RT, White RA, White EW, Weber JN, Roy D. The restoration of the articular surfaces overlying replamineform porous biomaterials. J Biomed Mater Res 1977;11:165–178.
12. Suominen E, Aho AJ, Vedel E, Kangasniemi I, Uusipaikka E, Yli-Urpo A. Subchondral bone and cartilage repair with bioactive glasses, hydroxyapatite, and hydroxyapatite-glass composite. J Biomed Mater Res 1996;32:543–551.
13. Cui JH, Park K, Park SR, Min BH. Effects of low-intensity ultrasound on chondrogenic differentiation of mesenchymal stem cells embedded in polyglycolic acid: An *in vivo* study. Tissue Eng 2006;12:75–82.
14. Lisignoli G, Cristino S, Piacentini A, Zini N, Noel D, Jorgensen C, Facchini A. Chondrogenic differentiation of murine and human mesenchymal stromal cells in a hyaluronic acid scaffold: Differences in gene expression and cell morphology. J Biomed Mater Res A 2006;77:497–506.
15. Banu N, Tsuchiya T. Markedly different effects of hyaluronic acid and chondroitin sulfate-A on the differentiation of human articular chondrocytes in micromass and 3-D honeycomb rotation cultures. J Biomed Mater Res A 2007;80:257–267.
16. Wozney JM, Rosen V, Celeste AJ, Mitsock LM, Whitters MJ, Kriz JM, Hewick RM, Wang EA. Novel regulators of bone formation: Molecular clones and activities. Science 1988;242:1528–1534.
17. Rosen V, Wozney JM, Wang EA, Cordes P, Celeste A, McQuaid D, Kurtzberg L. Purification and molecular cloning of a novel group of BMPs and localization of BMP mRNA in developing bone. Conn Tiss Res 1989;20:313–319.
18. Celeste AJ, Iannazzi JA, Taylor RC, Hewick RM, Rosen V, Wang EA, Wozney JM. Identification of transforming growth factor β family members present in bone-inductive protein purified from bovine bone. Proc Natl Acad Sci USA 1990;87:9843–9847.
19. Centrella M, Horowitz MC, Wozney JM, McCarthy TL. Transforming growth factor-β gene family members and bone. Endocrine Rev 1994;15:27–39.
20. Denker AE, Haas AR, Nicoll SB, Tuan RS. Chondrogenic differentiation of murine C3H10T1/2 multipotential mesenchymal cells: I. Stimulation by bone morphogenetic protein-2 in high-density micromass cultures. Differentiation 1999;64:67–76.
21. Li WJ, Tuli R, Okafor C, Derfoul A, Danielson KG, Hall DJ, Tuan RS. A three-dimensional nanofibrous scaffold for cartilage tissue engineering using human mesenchymal stem cells. Biomaterials 2005;26:599–609.
22. Masuda S, Yoshihara Y, Muramatsu K, Wakebe I. Repairing of osteochondral defects in joint using β-TCP / carboxymethyl chitin composite. Key Eng Mater 2005;284:791–794.
23. Kariya H, Kiyohara A, Masuda S, Yoshihara Y, Ueno M, Hashimoto M, Suda Y. Biological roles of carboxymetyl-chitin associated for the growth factor production. J Biomed Mater Res A 2007:83:58–63.
24. Shi Y, Massague J. Mechanisms of TGF-beta signaling from cell membrane to the nucleus. Cell 2003;113:685–700.
25. Newman SA. Lineage and pattern in the developing vertebrate limb. Trends Clenet 1988;4:329–332.
26. Hall BK, Miyake T. The membranous skeleton: The role of cell condensations in vertebrate skeletogenesis. Annt Embryol (Berl) 1992;186:107–124.
27. Zhang X, Ziran N, Gouter JJ, Sehwarz EM, Puzas JE, Rosier RN, Zuscik M, Drissi H, O'Keefe RJ. Primary murine limb bud mescenchymal cells in long-term culture complete chondrocyte differentiation: TGF-beta Delays hypertrophy and PGE2 inhibits terminal differentiation. Bone 2004;34:809–817.
28. Denker AE, Nicoll SB, Tuan RS. Formation of cartilage-like spheroids by micromass cultures of murine C3H10T1/2 cells upon treatment with transforming growth factor-beta 1. Differentiation 1995;59:25–34.
29. Haas AR, Tuan RS. Chondrogenic differentiation of murine C3H10T1/2 multipotential mesenchymal cells: II. Stimulation by bone morphogenetic protein-2 requires modulation of N-cadherin expression and function. Differentiation 1999;64:77–89.
30. Song JJ, Aswad R, Kanaan RA, Rico MC, Owen TA, Barbe MF, Safadi FF, Popoff SN. Connective tissue growth factor (CTGF) acts as a downstream mediator of TGF-beta1 to induce mesenchymal cell condensation. J Cell Physiol 2007;210:398–410.
31. Tokura S, Nishi N, Tsutsumi A, Somorin O. Studies on chitin VIII. Some properties of water soluble chitin Derivatives. Polym J 1983;15:485–489.
32. Ahrens M, Ankenbauer T, Schroder D, Hollnagel A, Mayer H, Gross G. Expression of human bone morphogenetic protein-2 or 4 in murine mesenchymal progenitor cells induces differentiation into distinct mesenchymal cell lineages. DNA Cell Biol 1993;12: 871–880.
33. Rosenberq L. Chemical basis for the histological use of safranin O in the study of articular cartilage. J Bone Joint Surg Am 1971;53: 69–82.
34. van Sliedregt A, van Blitterswijk CA, Hesseling SC, Grote JJ, dcGroot K. The effect of the molecular weight of polylactic acid on *in vitro* biocompatibility. Adv Biomater 1990;9:207–212.
35. Athanasion KA, Niederauer GG, Agrawal CM. Sterilization, toxicity, biocompatibility and clinical applications of polylactic acid/ polyglycolic acid copolymers. Biomaterials 1996;17:93–102.
36. Freed LE, Marquis JC, Nohria A, Emmanual J, Mikos AG, Langer R. Neocartilage formation *in vitro* and *in vivo* using cells cultured on synthetic biodegradable polymers. J Biomed Mater Res 1993; 27:11–23.
37. Meinel L, Hofmann S, Karageorgiou V, Kirker-Head C, McCool J, Gronowicz G, Zichner L, Langer R, Vunjak-Novakovic G, Kaplan DL. The inflammatory responses to silk films *in vitro* and *in vivo*. Biomaterials 2005;26:147–155.
38. Li H, Schwartz NB. Gene structure of chick cartilage chondroitin sulfate proteoglycan (aggrecan) core protein. J Mol Evol 1995;41: 878–885.
39. Watanabe H, Yamada Y, Kimata K. Roles of aggrecan, a large chondroitin sulfate proteoglycan, in cartilage structure and function. J Biochem 1998;124:687–693.
40. Sekiya I, Tsuji K, Koopman P, Watanabe H, Yamada Y, Shinomiya K, Nifuji A, Noda M. SOX9 enhances aggrecan gene promoter/ enhancer activity and is up-regulated by retinoic acid in a cartilage-derived cell line, TC6. J Biol Chem 2000;275: 10738–10744.
41. Bayliss MT, Howat S, Davidson C, Dudhia J. The organization of aggrecan in human articular cartilage. Evidence for age-related changes in the rate of aggregation of newly synthesized molecules. J Biol Chem 2000;275:6321–6327.
42. Roark EF, Greer K. Transforming growth factor-beta and bone morphogenetic protein-2 act by distinct mechanisms to promote chick limb cartilage differentiation *in vitro*. Dev Dyn 1994;200: 103–116.
43. Watanabe H, de Caestecker MP, Yamada Y. Transcriptional cross-talk between Smad, ERK1/2, and p38 mitogen-activated protein kinase patyways regulates transforming growth factor-beta-induced

aggrecan gene expression in chondrogenic ATDC5 cells. J Biol Chem 2001;276:14466–14473.
44. Schmitt B, Ringe J, Haupl T, Notter M, Manz R, Burmester G-R, Sittinger M, Kaps C. BMP2 initiates chondrogenic lineage development of adult human mesenchymal stem cells in high-density culture. Differentiation 2003;71:567–577.
45. Tanaka H, Murphy CL, Murphy C, Kimura M, Kawai S, Polak JM. Chondrognic differentiation of murine embryonic stem cells: effects of culture conditions and dexamethasone. J Cell Biochem 2004;93:454–462.
46. zur Nieden NI, Kempka G, Rancourt DE, Ahr HJ. Induction of chondro-, osteo-, and adipogenesis in embryonic stem cells by bone morphogenetic protein-2: Effect of cofactors on differentiating lineages. BMC Dev Biol 2005;5:1
47. Tuli R, Tuli S, Nandi S, Huang X, Manner PA, Hozack W, Danielson KG, Hall DJ, Tuan RS. Transforming growth factor-β-mediated chondrogenesis of human mesenchymal progenitor cells involves N-cadherin and mitogen-activated protein kinase and Wnt signaling cross-talk. J Biol Chem 2003;278:41227–41236.
48. Lefebvre V, Huanq W, Harlev VR, Goodfellow PN, de Crombruqqhe B. Sox9 is a potent activator of the chondrocyte-specific enhancer of the pro alpha1(II) collagen gene. Mol Cell Biol 1997; 17:2336–2346.
49. Kulyk WM, Franklin JL, Hoffman LM. Sox9 expression during chondrogenesis in micromass cultures of embryonic limb mesenchyme. Exp Cell Res 2000;255:327–332.
50. Aszodi A, Hunziker EB, Olsen BR, Fassler R. The role of collagen II and cartilage fibril-associated molecules in skeletal development. Osteoarthritis Cartilage 2001;9:150–159.
51. Gustafsson E, Aszdi A, Orteqa N, Hunziker EB, Denker HW, Werb Z, Fassler R. Role of collagen type II and perlecan in skeletal development. Ann N Y Acad Sci 2003;995:140–150.
52. Bosnakovski D, Mizuno M, Kim G, Takaqi S, Okumura M, Fujinaqa T. Chondrogenic differentiation of bovine bone marrow mexenchymal stem cells (MSCs) in different hydrogels: Influence of collagen type II extracellular matrix on MSC chondrogenesis. Biotechnol Bioeng 2006;93:1152–1163.
53. Williams CG, Kim TK, Taboas A, Manson P, Elisseeff J. In vitro chondrogenesis of bone marrow-derived mesenchymal stem cells in a photopolymerizing hydrogel. Tissue Eng 2003;9:679–688.
54. Huang JI, Zuk PA, Jones NF, Zhu M, Lorenz HP, Hedrick MH, Benhaim P. Chondrogenic potential of multipotential cells from human adipose tissue. Plast Reconstr Surg 2004;113:585–594.
55. Hedbom E, Antonsson P, Hierpe A, Aeschimann D, Paulsson M, Rosa-Pimentel E, Sommarin Y, Wendel M, Oldberg A, Heinegard D. Cartilage matrix proteins. An acidic oligomeric protein (COMP) detected only in cartilage. J Biol Chem 1992;267:6132–6136.
56. Halasz K, Kassner A, Morqelin M, Heineqard D. COMP acts as a catalyst in collagen fibrillogenesis. J Biol Chem 2007;282: 31166–31173.
57. Kipnes J, Carlberg AL, Loredo GA, Lawler J, Tuan RS, Hall DJ. Effect of cartilage oligomeric matrix protein on mesenchymal chondrogenesis *in vitro*. Osteoarthritis Cartilage 2003;11:442–454.
58. Liu CJ, Prazak L, Fajardo M, Yu S, Tyagi N, Di Cesare PE. Leukemia/lymphoma-related factor, a POZ domain-containing transcriptional repressor, interacts with histone deacetylase-1 and inhibits cartilage oligomeric matrix protein gene expression and chondrogenesis. J Biol Chem 2004;279:47081–47091.
59. Chen AL, Frang C, Liu C, Leslie MP, Chang E, Di Cesare PE. Expression of bone morphogenetic proteins, receptors, and tissue inhibitors in human fetal, adult, and osteoarthritic articular cartilage. J Orthop Res 2004;22:1188–1192.
60. Im GI, J NH, Tae SK. Chondrogenic differentiation of mesenchymal stem cells isolated from patients in late adulthood: The optimal conditions of growth factors. Tissue Eng 2006;12:527–536.
61. Mehlhorn AT, Schmal H, Kaiser S, Lepski G, Finkenzeller G, Stark GB, Sudkamp NP. Mesenchymal stem cells maintain TGF-beta-mediated chondrogenic phenotype in alginate bead culture. Tissue Eng 2006;12:1393–1403.
62. K Yasuda, N Kitamura, JP Gong, K Arakaki, HJ Kwon, S Onodera, YM Chen, T Kurokawa, F Kanayam, Y Ohmiya, Y Osada. A novel double-network hydrogel induces spontaneous articular cartilage regeneration *in vivo* in a large osteochondral defect. Macromol Biosci 2009;9:307–316.

# Role of Human Herpes Virus 6 in Corneal Inflammation Alone or With Human Herpesviruses

*Toshiomi Okuno, MD, PhD,* Laura C. Hooper, PhD,† Roxana Ursea, MD,‡ Janine Smith, MD,‡ Robert Nussenblatt, MD,†‡ John J. Hooks, PhD,† and Kozaburo Hayashi, MD, PhD†*

**Purpose:** The purpose of this study was to determine the association of human herpes virus 6 (HHV-6) and/or other human herpesviruses in corneal inflammation using polymerase chain reaction (PCR).

**Methods:** We collected tear films, conjunctival smears, and a corneal button of inflamed cornea, and the presence of HHV-6 and other herpesviruses in these samples were assessed by a nested PCR.

**Results:** In tear films collected from 3 of 9 patients with dendritic keratitis, HHV-6 DNA was positive twice, together with herpes simplex virus (HSV) or varicella zoster virus DNA most often, during the acute phase of the disease. Two other patients in this group were either positive for HSV-1 and varicella zoster virus or for HSV-1 and Epstein–Barr virus DNA but negative for HHV-6. When another 12 patients' smear samples from corneal ulcer or keratouveitis were examined, 9 were positive for HHV-6 DNA. Of these, 4 were positive for HSV-1 simultaneously, whereas the remaining 5 patients were negative for HSV-1. One patient's smear was positive for HSV-1 but not for HHV-6. In the corneal button, both HSV and HHV-6 DNAs were positive by nested PCR. HHV-6 was also positive by nested PCR in the conjunctival swab obtained from the contralateral inflamed eye of the patient.

**Conclusions:** In 22 patients with corneal inflammation, HHV-6 was positive in 14 of 22 patients and HSV-1 was found in 9 of those patients. These data indicated that the association of HHV-6 with disease was more frequent than with other herpesviruses and that HHV-6 may be another sole causative agent for corneal inflammation.

**Key Words:** human herpesvirus 6, herpes simplex virus, varicella zoster virus, cornea, inflammation, polymerase chain reaction

(*Cornea* 2011;30:204–207)

Received for publication November 13, 2009; revision received March 9, 2010; accepted March 25, 2010.

From the *Department of Microbiology, Hyogo College of Medicine, Hyogo, Japan; †Laboratory of Immunology, Research Institute; and ‡Ophthalmology Clinic, National Eye Institute, National Institute of Health, Bethesda, MD.

Supported (in part) by the Intramural Research Program of the National Eye Institute, National Institutes of Health.

Reprints: Toshiomi Okuno, Department of Microbiology, Hyogo College of Medicine, 1-1, Mukogawa-cho, Nishinomiya, Hyogo 663-8501, Japan (e-mail: tmokuno@hyo-med.ac.jp).



Human herpesvirus 6 (HHV-6) was originally isolated from patients' peripheral blood mononuclear cells (PBMCs) with lymphoproliferative disorders and/or patients infected with human immunodeficiency virus in 1986.[1] HHV-6 is classified into 2 groups, variant A (HHV-6A) and variant B (HHV-6B) according to their antigenic and biological characteristics.[2] HHV-6B causes exanthem subitum (ES),[3] whereas HHV-6A–related disease is currently still unknown.

Herpetic keratitis caused by herpes simplex virus type 1 (HSV-1) is a vision-threatening disease. HSV-1 harbored in the trigeminal ganglion frequently reactivates and causes recurrent corneal herpes, which eventually leads to herpetic stromal keratitis (HSK) with dense stromal haze in some patients. Association of HHV-6 in ocular diseases has been amply documented in the literature in which presence of HHV-6 DNA in corneal tissues was described.[4,5]

In the present study, we collected tears, smears of conjunctival and corneal epithelium, and a corneal button. Presence of HSV-1, varicella zoster virus (VZV), and HHV-6 DNAs in these samples was assessed by nested polymerase chain reaction (PCR) to see if HHV-6 associates with HSV-1 or VZV.

## MATERIALS AND METHODS

### Sample Collection and DNA Extraction

The ethics committee of Hyogo College of Medicine and the National Cancer Institute and local institutional review boards approved the study. Tears were collected from 47 normal eyes, 10 eyes of patients with ES, and 9 eyes of patients with dendritic keratitis by the Schirmer method or by an aspiration of 50-μL saline instilled in the lower conjunctival sac. Conjunctival and corneal epithelial cells were scraped off from 12 patients with corneal ulcers or keratouveitis using a cotton swab. These samples were treated with buffered proteinase K at 60°C for 3 hours, then heated at 95°C to inactivate the enzymatic activity. A herpetic corneal button obtained during the corneal transplant performed in the Ophthalmology Clinic at the National Eye Institute (NEI) was cut in 8-μm thick specimens, which were boiled in sterile distilled water for 15 minutes. Supernatants of these treated samples were used as templates for a single PCR or a nested PCR amplification.

### Amplification of Viral DNA

Nested PCR for HHV-6 and dot blot hybridization of PCR products were performed as described previously.[6]

Briefly, 5 μL of each sample in a 45-μL reaction mixture containing outer primers and Taq polymerase was amplified for 30 cycles, composed of a denaturing step at 90°C for 1 minute, annealing at 62°C, and extension at 72°C for 3 minutes. Five microliters of the PCR product was then further amplified in the second round of PCR using nested primers. HHV-6A DNA, U1102 strain, and HHV-6B DNA, HST strain, served as positive controls. Electrophoresis of these PCR products was performed, and the obtained bands were size identified with ethidium bromide staining. To confirm the results further, transferred bands were hybridized with a corresponding alkaline phosphatase–conjugated oligonucleotide probe. Nested PCRs for HSV-1 were performed as described previously.[7] Briefly, 5 μL of DNAs purified from clinical samples was added to the reaction mixture containing Taq polymerase and outer primers, then amplified 40 cycles at 94°C for 1 minute, 55°C for 2 minutes, and 72°C for 1.5 minutes. Second round PCR was performed using nested primers at the same thermal cycling conditions. The corneal button and smear samples, obtained in the NEI Clinic, were subjected to nested PCR using the protocol by Mitchell et al.[7] Ten microliters of nested PCR product was run on a 4% agarose gel, transblotted to a nylon membrane, and hybridized with a specific internal HSV-1 or HHV-6 probe labeled with digoxigenin.

## RESULTS

In the tear films collected from 3 of 9 patients with herpetic dendritic keratitis, HHV-6 DNA was positive for 5 of 6 times together with HSV or VZV DNA during the acute phase of the disease (Table 1). HHV-6 and HSV-1 DNAs were detected on the first day of examination in patient 1. After treating her with a topical acyclovir, HSV-1 DNA disappeared on the following day from the tear film but HHV-6 remained positive. In patients 2 and 3 who had been diagnosed with pseudodendrite, tears were positive for VZV and HHV-6 DNAs. Patient 3 had facial eruptions of zoster. Both were treated with a topical acyclovir, and in patient 2, both viral DNAs disappeared after the initiation of the topical acyclovir applications. However, both viral DNAs remained positive in patient 3 even after treatment with topical acyclovir. Another patient was positive for HHV-6 DNA twice but negative for other herpesviruses. Two patients in this group were either positive for HSV-1 and VZV or for HSV-1 and Epstein–Barr virus DNAs but negative for HHV-6. Although the remaining 3 patients with other forms of keratitis were examined, they were negative for all herpesviruses examined. As a control, tears collected from 47 normal eyes and 10 patients with ES (57) were examined. None of them showed positive results for HHV-6.

We next examined 12 patients' smear samples, of which 8 were obtained from patients with corneal ulcer and 4 from patients with keratouveitis (Table 2). Among them, 9 PCR products were positive for HHV-6 (Fig. 1A) and were further identified as HHV-6B by dot blot hybridization (Fig. 1B). Of these 9 patients, 4 patients were positive for HSV-1 simultaneously. The remaining 5 patients were positive for HHV-6 but negative for HSV-1. One patient with corneal ulcer had a smear that was positive for HSV-1 but not for HHV-6. One patient with uveitis and another patient with corneal ulcer were negative for both viruses. In the corneal button obtained from a patient in the NEI Clinic, who was living in the United States, both HSV and HHV-6 DNAs were positive by nested PCR (Fig. 2). HHV-6 was also positive by nested PCR in the conjunctival swab obtained from the contralateral inflamed eye of the patient (Fig. 2). During the follow-up study, HHV-6 was not detected in the patient's tears and conjunctival swabs at 2 weeks after the corneal allograft transplantation but it was positive in saliva at 4 weeks after the corneal graft operation (data not shown).

## DISCUSSION

We evaluated 22 patients with corneal inflammation. Among them, HHV-6 was positive in 14 of 22 patients and HSV-1 was found in 9 of those patients. Only 5 patients were negative for herpesvirus DNA. These results indicated that the majority of the corneal inflammation was correlated with herpesviruses and that the association of HHV-6 with disease was more frequent than with other herpesviruses. In contrast, HHV-6 DNA was not detected in 47 tear samples obtained from normal individuals and in the 10 tear samples obtained

**TABLE 1.** Detection of Herpesvirus DNA in Tear Films

| | Time (D) | Symptom | Treatments | Positive PCR |
|---|---|---|---|---|
| Patient 1 | 0 | DK | ACV | HHV-6, HSV-1 |
| (37 yr, female) | 1 | DK, herpes labialis | ACV | HHV-6 |
| Patient 2 | 0 | DK | — | HHV-6, VZV |
| (78 yr, female) | 3 | DK | ACV | HHV-6, VZV |
| | 9 | Cure | IDU | (−) |
| | 41 | — | IDU | (−) |
| Patient 3 | 0 | Zoster, keratitis | ACV | HHV-6, VZV |
| (77 yr, male) | 3 | DK | ACV | HHV-6, VZV |

ACV, acyclovir; DK, dendritic keratitis; IDU, idoxuridine.

**TABLE 2.** Detection of Herpesvirus DNA in Patients With Corneal Ulcer and Keratouveitis

| Patient | HHV-6 | HSV-1 | Others | Diagnosis |
|---|---|---|---|---|
| 1 | + | + | − | UC |
| 2 | + | + | − | UC |
| 3 | + | + | − | UC |
| 4 | + | + | − | KU |
| 5 | + | − | − | UC |
| 6 | + | − | − | UC |
| 7 | + | − | − | UC |
| 8 | + | − | − | KU |
| 9 | + | − | − | KU |
| 10 | − | + | − | UC |
| 11 | − | − | − | UC |
| 12 | − | − | − | KU |

+, PCR positive; −, PCR negative; KU, keratouveitis; UC, ulcer of the cornea.

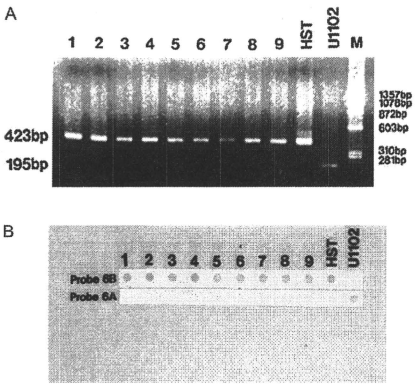


**FIGURE 1.** A, Agarose gel electrophoresis of 9 PCR-positive samples. U1102 and HST are representative strains of HHV-6A and HHV-6B, respectively. M, molecular size markers. B, Dot blot hybridization of 9 PCR-positive samples with variant A–specific (probe 6A) and variant B–specific (probe 6B) probes. All 9 samples amplified by nested PCR were variant B by size and hybridization with probe 6B.

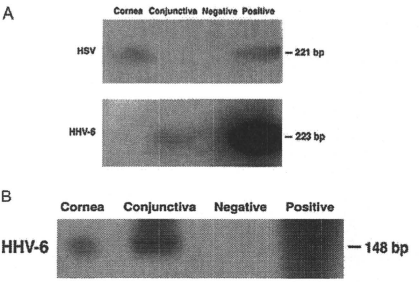


**FIGURE 2.** A, Detection of HSV and HHV-6 in a patient's sample by PCR. Samples were subjected to PCR followed by gel electrophoresis. Bands were transblotted onto nylon membranes and confirmed by hybridization with specific internal HSV and HHV-6 probes. B, Detection of HHV-6 in a patient's sample by nested PCR. Samples were subjected to nested PCR followed by gel electrophoresis. Transblotted bands were hybridized with a specific HHV-6 probe. Negative, negative control; Positive, positive control.

from patients with ES. Because patients with ES usually present without ocular symptoms and HHV-6 DNA was not detected in patients' secretions such as saliva shortly after onset of the disease as indicated by Suga et al,[8] these results were not unexpected. Two possibilities can be drawn from the results of these PCR analyses. First, HHV-6 is a causal agent of keratitis because in 1 tear and 5 swab samples from 9 patients with dendritic keratitis and 12 patients with corneal ulcer, respectively, HHV-6 DNA was singly detected. Second, HHV-6 reactivates and is associated with the lesions caused by HSV or other agents.

In total, 8 of 15 samples where HHV-6 DNAs were found, other herpesvirus DNAs were also found. Qavi et al[9] reported the possible worsening and long-lasting role of HHV-6 in herpetic keratitis in rabbit. They also found HHV-6 antigens, transcripts, and DNA sequences in the corneal buttons collected from patients infected with human immunodeficiency virus 1 at autopsy.[4,5] In addition, they showed HHV-6 in a few samples of a CCRF-HSB2 T cell line. This cell line is known to support only HHV-6A growth. Most of the HHV-6A strains were detected or isolated from patients with AIDS, whereas all the HHV-6 detected in other immunocompromized patients were variant B.

Robert et al[10] also detected both HHV-6 and HSV-1 DNAs in the tear film from a patient with dendritic keratitis. Recent evidence suggests that HHV-6 infection creates an immunosuppressive milieu. In the fatal immune suppression associated with disseminated HHV-6 infection, patients lack proliferation of antigen specific T lymphocytes.[11,12] Although the mechanisms of HHV-6–induced immune suppression are still largely unknown, several types of evidence have been reported, including the inhibition of interleukin (IL)-12 p70 production by macrophages,[13] a defective antigen presentation, nonmaturation of dendritic cells,[14] and aberrant cytokine production.[11,15–17] We recently found that in HHV-6 infection, $CD4^+CD25^{high}$ regulatory T cells suppressed conventional T cells via enhanced IL-10 production.[18] Arena et al[15] reported that PBMCs infected with HHV-6 upregulate IL-10 and downregulate interferon γ production upon lipopolysaccharide stimulation. HHV-6 also inhibits IL-2 release from PBMCs and $CD3^+$ and $CD4^+$ T cells. Wang et al[19] suggested that IL-10 produced by HHV-6-stimulated $CD4^+$ T cells obtained from HHV-6–uninfected individuals suppressed naive $CD4^+$ and $CD8^+$ T-cell activity. Thus, HHV-6 may enhance disease severity because of its immunosuppressive effect by facilitating HSV-1 replication. In contrast, it may be just a bystander because when HSV-1 causes corneal inflammation, infiltrating T cells or macrophages may carry HHV-6. To answer this question we have to get more clinical samples with clear clinical findings. However, we also observed HHV-6 DNA but not HSV-1 DNA results in the smear samples from 5 of 12 patients (Table 2). These data indicate that HHV-6 may be another causative agent by itself for corneal inflammation. In addition, it is not clear how the resolution of the disease changes the HHV-6 status. Because we did not get the sample after resolution of the disease, further observation and laboratory tests are necessary in the future.

## REFERENCES

1. Salahuddin SZ, Ablashi DV, Markham PD, et al. Isolation of a new virus, HBLV, in patients with lymphoproliferative disorders. *Science*. 1986;234:596–600.
2. Ablashi DV, Balachandran N, Josephs SF, et al. Genomic polymorphism, growth properties, and immunologic variations in human herpesvirus-6 isolates. *Virology*. 1991;184:545–552.

3. Yamanishi K, Okuno T, Shiraki K, et al. Identification of human herpesvirus-6 as a causal agent for exanthem subitum. *Lancet*. 1988;1:1065–1067.
4. Qavi HB, Green MT, SeGall GK, et al. The incidence of HIV-1 and HHV-6 in corneal buttons. *Curr Eye Res*. 1991;10(Suppl):97–103.
5. Qavi HB, Green MT, SeGall GK, et al. Frequency of dual infections of corneas with HIV-1 and HHV-6. *Curr Eye Res*. 1992;11:315–323.
6. Okuno T, Oishi H, Hayashi K, et al. Human herpesvirus 6 and 7 in cervixes of pregnant women. *J Clin Microbiol*. 1995;33:1968–1970.
7. Mitchell SM, Fox JD, Tedder RS, et al. Vitreous fluid sampling and viral genome detection for the diagnosis of viral retinitis in patients with AIDS. *J Med Virol*. 1994;43:336–340.
8. Suga S, Yazaki T, Kajita Y, et al. Detection of human herpesvirus 6 DNAs in samples from several body sites of patients with exanthem subitum and their mothers by polymerase chain reaction assay. *J Med Virol*. 1995;46:52–55.
9. Qavi HB. Possible role of HHV-6 in the enhanced severity of HSV-1 keratitis. *In Vivo*. 1999;13:427–432.
10. Robert PY, Traccard I, Adenis JP, et al. Multiplex detection of herpesviruses in tear fluid using the "stair primers" PCR method: prospective study of 93 patients. *J Med Virol*. 2002;66:506–511.
11. Flamand L, Gosselin J, Stefanescu I, et al. Immunosuppressive effect of human herpesvirus 6 on T-cell functions: suppression of interleukin-2 synthesis and cell proliferation. *Blood*. 1995;85:1263–1271.
12. Knox KK, Pietryga D, Harrington DJ, et al. Progressive immunodeficiency and fatal pneumonitis associated with human herpesvirus 6 infection in an infant. *Clin Infect Dis*. 1995;20:406–413.
13. Smith A, Santro F, Di Lullo G, et al. Selective suppression of IL-12 production by human herpesvirus 6. *Blood*. 2003;102:2877–2884.
14. Kakimoto M, Hasegawa A, Fujita S, et al. Phenotypic and functional alterations of dendritic cells induced by human herpevirus 6 infection. *J Virol*. 2002;76:10338–10345.
15. Arena A, Liberto MC, Iannello D, et al. Altered cytokine production after human herpes virus type 6 infection. *New Microbiol*. 1999;22: 293–300.
16. Flamand L, Gosselin J, D'Addario M, et al. Human herpesvirus 6 induces interleukin-1 beta and tumor necrosis factor alpha, but not interleukin-6, in peripheral blood mononuclear cell cultures. *J Virol*. 1991;65:5105–5110.
17. Smith A.P, Paolicci C, Di Lullo G, et al. Viral replication-independent blockade of dendritic cell maturation and interleukin-12 production by human herpesvirus 6. *J Virol*. 2005;79:2807–2813.
18. Otani N, Okuno T. Human herpesvirus 6 infection of $CD4^+$ T-cell subsets. *Microbiol Immunol*. 2007;51:993–1001.
19. Wang F, Yao K, Yin QZ, et al. Human herpesvirus-6-specific interleukin 10-producing $CD4^+$ T cells suppress the $CD4^+$ T-cell response in infected individuals. *Microbiol Immunol*. 2006;50:787–803.

Med Chem Res (2010) 19:1273–1286
DOI 10.1007/s00044-009-9269-6

MEDICINAL CHEMISTRY RESEARCH

ORIGINAL RESEARCH

# Use of structure-based virtual screening in the investigation of novel human sialidase inhibitors

**Sadagopan Magesh · Setsuko Moriya · Tohru Suzuki · Taeko Miyagi · Hideharu Ishida · Makoto Kiso**

Received: 13 May 2009 / Accepted: 16 September 2009 / Published online: 14 October 2009


**Abstract** Recent studies have determined the molecular mechanisms underlying the pathological alterations of sialic acid or its conjugates in various human disease states, and the sialic acid modifying enzyme sialidase has been adopted as an attractive therapeutic option for diseases like cancer, diabetes, inflammation, and arteriosclerosis. Isoform human sialidase inhibitors are also a good chemical tool for exploring the differential functions of human sialidases. In the current study, structure-based virtual screening was attempted to identify the compounds containing novel structures for human sialidase inhibition. The best-hit compound, containing a furan core structure with a dicarboxylic acid group, was purchased from Maybridge Chemical Company and was evaluated for its inhibitory activity against all four types of sialidases. This is the first report on the structure-based virtual screening of human sialidases and provides some structural insights for further efforts in this area.

**Keywords** Sialic acid · Sialidase · Virtual screening · Inhibitor design · Docking

S. Magesh (✉) · H. Ishida · M. Kiso (✉)
Department of Applied Bioorganic Chemistry, Faculty of Applied Biological Sciences, Gifu University, Yanagido 1-1, Gifu, Gifu 501-1193, Japan
e-mail: sadagopan_magesh@yahoo.com

M. Kiso
e-mail: kiso@gifu-u.ac.jp

S. Moriya · T. Miyagi
Department of Biochemistry, Miyagi Cancer Center Research Institute, Miyagi, Japan

T. Suzuki
The United Graduate School of Agricultural Sciences, Gifu University, Yanagido 1-1, Gifu, Japan

S. Magesh · M. Kiso
Institute for Integrated Cell-Material Sciences (iCeMS), Kyoto University, Kyoto, Japan

## Introduction

Sialic acids (**1**) are a unique family of sugars with a nine-carbon skeleton and a carboxylic acid. They are not ubiquitous in nature but do exist in the deuterosome lineage of animals, but not in plants, prokaryotes, or most invertebrates (Corfield and Schauer, 1982). Given their terminal location and diversity, sialic acids play crucial roles in various biological processes by influencing the chemical and biological features of several classes of cell surface and secreted glycan molecules (Schauer *et al.*, 1995). Most importantly, the presence and absence of sialic acid and its recognizing proteins have been excogitated in human evolution. Altered levels of sialic acids have been correlated with various pathological conditions such as tumourogenesis, inflammation, and hyperlipidemia. Sialic acids also act as a virulence factor for many pathogens like virus, bacteria, and protozoa (Schauer, 2000).

Sialidases have also been known as exo-α-sialidases; they desialylate the terminal sialic acid residues from glycoproteins, glycopeptides, gangliosides, oligosaccharides, and polysaccharides. They are mainly involved in the degradation of sialoglycoconjugates and therefore regulate cellular processes by modifying the sialic acid content in the cell (Saito and Yu, 1995). Sialidase are thought to be involved in various biological processes like cell growth, cell proliferation, cell differentiation, cell migration, cellular transport, signal transduction, antigen masking, inter and intra cell interactions, and infection (Achyuthan and Achyuthan, 2001). Many of these cellular functions could be secondary to the desialylation effect of sialidase, and in some cases direct involvement of sialidases has been proposed (Schauer, 1985). Sialidases are widely distributed among different classes of organisms, from echinoderm to mammals, and, also, in some microbes such as viruses, bacteria, and protozoa, even though most of them lack sialic acids (Miyagi and Yamaguchi, 2008).

Sialidases of mammalian origin have been implicated in the modulation of various functional molecules involved in many biological processes, whereas the functions of their microbial orthologues appear only to be limited to nutrition and pathogenesis (Schauer, 2000). The four types of mammalian sialidases have been cloned and classified according to their major intracellular location. In human, they are designated intralysosomal sialidase (NEU1), cytosolic sialidase (NEU2), plasma membrane-associated sialidase (NEU3), and lysosomal or mitochondrial membrane-associated sialidase (NEU4). These sialidase isoforms (NEUs) also differ in enzymatic properties including substrate specificities and immunological properties (Miyagi *et al.*, 2004a, b). Aberrant expression of human sialidases has been found to be associated with the development of various pathological conditions (Miyagi and Yamaguchi, 2008; Igdoura *et al.*, 2007; Sasaki *et al.*, 2003). Particularly, NEU3 was found to be significantly up-regulated in various human cancers and its up-regulation was correlated with suppression of apoptosis and promotion of motility in cancer cells. Polymorphism of the NEU3 gene in diabetic patients was discovered and found to be deeply involved in the onset of Type II diabetes (Miyagi *et al.*, 2007). Suppression of NEU1 expression reduced the levels of cholesterol associated with atherogenic lipoproteins (VLDL, IDL, LDL), but not protective lipoproteins (HDL), and also suppressed the development of atherosclerosis. The efficacy of the

use of a sialidase inhibitor as an agent for the treatment of high-LDL cholesterol or triglycerides and cardiovascular disease, diabetes, and related diseases was recently demonstrated in animal models (Igdoura *et al.*, 2007). These studies suggest that sialidase might play important etiological and pathogenic roles in the above-mentioned disease states. Indeed, sialidase is a new risk factor, and treatment with sialidase inhibitors is a novel therapeutic approach in these disease states. Importantly, identification of selective inhibitors for each isoform that can be used as probes can clarify the molecular basis of individual human sialidase functions. For instance, no clear-cut information is available on the type of sialidase(s) involved in the sialidase activity of human T lymphocytes (Hata *et al.*, 2008).

To date, about 150 crystal structures of sialidases from various species are available in the protein data bank. Fourteen crystal structures of human cytosolic sialidase (NEU2) were resolved with or without ligand. Structural comparisons of viral, bacterial, protozoal, and human sialidases have revealed a common canonical six-blade $\beta$-propeller arrangement despite their lower sequence similarity (<30%), and variations are typically found in the twist of $\beta$-stands and their connecting loops (Chavas *et al.*, 2005). The structure-based design of viral sialidase inhibitors has led to a new class of antiviral drugs for influenza fever (Von Itzstein *et al.*, 1993). Microbial sialidases from other various sources (e.g., *Trypanosoma cruzi, Vibrio cholerae*) have also been considered as targets for therapeutic invention (Mann *et al.*, 2006; Neres *et al.*, 2007). In a previous study, we modeled structures of NEU1, NEU3, and NEU4 using the crystal structure of NEU2 in complex with the nonspecific inhibitor DANA (2-deoxy-2,3-dehydro-i-acetylneuraminic acid; Neu5Ac2en; **2**) and pointed out the putative active site amino acid residues that form the specificity pocket (Magesh *et al.*, 2006). In our initial approach, we designed a series of C9 amide-linked hydrophobic derivatives of DANA that extend to the specificity pocket and achieved at least 100-fold selectivity for NEU1 over NEU2, NEU3, and NEU4 with **3** (GSC-649) (Fig. 1) (Magesh *et al.*, 2008). Then we applied structure-based methods to generate novel inhibitor scaffolds, away from the sugar framework, which are readily available or synthetically accessible for in vitro screening. Through a de novo-based approach, we designed fluorobenzoic acid derivatives, and marginal NEU2 selectivity was attained with compound **4**, GSC-697 (Magesh *et al.*, 2009). In the present study, we report the structure-based virtual screening of a Maybridge Chemical Co. database against the crystal structure of NEU2, which suggested a series of novel structures for sialidase inhibition. The best-scored hit (**5**) was purchased and screened against all four types of human sialidases. Though compound **5** has exhibited weak inhibitory activities against human sialidases, its structural features have provided some promising information for further design and, also, on its potential activity against viral, bacterial, and parasitic sialidases.

## Experimental

All computations and simulations were carried out on an Intel P4-based Microsoft Windows 2000 workstation using the Discovery Studio Modeling 1.5 Package (Accelrys Inc., San Diego, CA, USA).

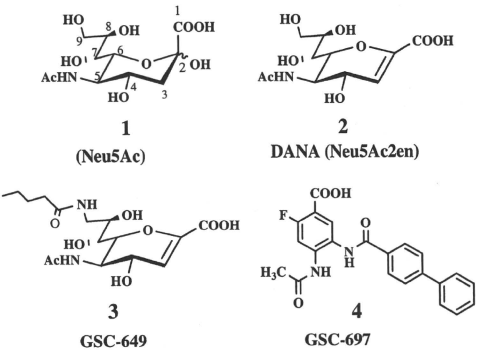


**Fig. 1** Structures of a common sialic acid, **1** (Neu5Ac); the nonspecific inhibitor DANA, **2** (Neu5Ac2en); **3** (GSC-649); and **4** (GSC-697)

## Virtual screening protocol

The crystal structure of the NEU2-DANA complex (PDB entry 1VCU, chain B) was used for virtual screening (Chavas *et al.*, 2005). Before docking, hydrogen atoms were added to the protein structure and the atom types were assigned by CHARMM force field. 4-Morpholine ethanesulfonic acid (MES) and all water molecules were removed from the protein structure. The bound ligand was used to define the active site for the docking run, with residues within 8 Å of the bound inhibitor included in the active-site definition. The active site included residues Arg21, Ile22, Arg 41, Asp46, Met85, Asn86, Ile103, Ile105, Thr122, Thr156, Ala158, Tyr179, Tyr181, Pro192, Leu217, Glu218, Arg237, Gln270, Arg304, and Tyr334. Leu115 and Glu111 were not included in the active-site definition. To determine whether the residues were assigned the correct protonation states, all the Arg, Lys, Asp, and Glu residues were visually inspected. The Maybridge database library of about 72,766 (in three sets: 28,614 + 26,928 + 17,222) compounds was docked flexibly into the active site using the DS LigandFit Module (Venkatachalam *et al.*, 2003). The database was collected from the ZINC database (Version 7), a free database of commercially available compounds for virtual screening (Irwin and Shoichet, 2005). The bound inhibitor was not included in the docking run. Some docking options were set to default conditions, such as force field (Dreiding) grid extension (3.0), nonbonded cutoff distance (10), softened potential energy (True), distance-dependent dielectric constant (1), Monte Carlo options for ligand conformational space, pose optimization, shape filtering, pose filtering, postprocessing, etc. The maximum number of poses retained was fixed to one and thresholds for diversity of saved poses were set based on scoring functions. Dock score, LigScore2, LUDI energy estimate 3, PLP2, Jain, and PMF were used as scoring functions. Initial hits were subjected to various step-by-step criteria such as Dock score ($\geq$50), consensus scoring, binding orientation, and scaffold basis to come up finally with the final 13

hits for further evaluation. Redocking of hit **5** into all four human sialidases was attempted as reported elsewhere. The electrostatic potential around the surface of the ligand was calculated using a solvent probe radius of 1.4 Å.

### Biological assay

Sialidase inhibition activity was performed according to previously reported procedures (Hata *et al.*, 2008). The hit compound (**5**; 3,4-di(benzyloxy) furan-2,5-dicarboxylic acid; Cat. Ref. BTB10004) was purchased from Maybridge Chemical Company (Trevillet; Tintagel, Cornwall, UK). Inhibitory activities were determined using homogenates obtained from HEK-293 cells transiently transfected with the expression plasmid containing a full-length human sialidase cDNA. Cells were sonicated in 9 vol of PBS, pH 7.4, containing 1 mM EDTA, 0.5 mM PMSF, 10 μg/ml leupeptin, and 0.5 μg/ml pepstatin, and centrifuged at 1000 *g* for 10 min. The supernatant (crude extract) was used for sialidase assays. Briefly, the routine reaction mixture contained 10–20 nmol of substrate as bound sialic acid, 0.2 mg of BSA, 10 μmol of sodium acetate (pH 4.6), and 0.2 mg of Triton X-100. After incubation at 37°C for 10–30 min, the amount of sialic acid released was determined fluorometrically. Sialidase activity with 4MU-NeuAc (NEU1, NEU2, and NEU4) as substrate was assayed by spectrofluorometric measurement of 4-methylumbelliferone released. In the case of NEU3, mixed ganglioside was used as a substrate and sialic acid released from ganglioside was measured by fluorometric HPLC with malononitrile. One unit of sialidase was defined as the amount of enzyme cleaving 1 nmol of sialic acid per hour. Compound **5** was tested at concentrations $\leq$1 mM. $IC_{50}$ values from concentration-inhibition curves were calculated by means of nonlinear regression analysis using Microsoft Excel 2000.

## Results and discussion

Virtual screening or virtual high-throughput screening is a computer-based technology that is gaining impetus in inhibitor discovery. It involves the rapid assessment of large libraries of chemical structures in order to guide the selection of likely ligand candidates. Thus, it can be an excellent way to save time and resources in the search for new lead compounds. Virtual screening encompasses a variety of sequential computational phases, including target and database preparation, docking and postdocking analysis, and prioritization of compounds for testing (Kitchen *et al.*, 2004) (Fig. 2). As we aimed to discover the novel scaffold(s) for human sialidase inhibition, we sought to utilize the crystal structure of NEU2 in complex with DANA (PDB entry 1VCU, chain B), as it is experimentally resolved among human sialidases (Chavas *et al.*, 2005). The active site was defined as a subset that contains 20 residues, in which any atom lies within 8 Å from DANA. Residues Leu115 and Glu111 were not included in the active-site definition to preserve the open conformation of the active site. The ligand sets (total of 72,766) from Maybridge Chemical Co. were downloaded from the ZINC database, which is a free database of commercially available compounds that contains more than 8 million

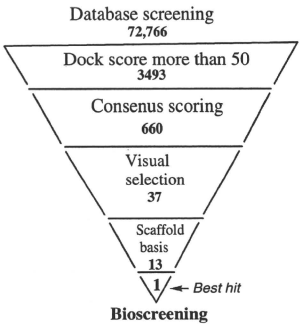


**Fig. 2** Virtual screening cascade

purchasable compounds in ready-to-dock, three-dimensional formats (Venkatachalam *et al.*, 2003). The Ligandfit docking program was used to dock the flexible ligand sets into a rigid receptor model. LigandFit docks small molecule ligands into protein active sites by considering the shape complementarity between the ligand and the protein active site and estimates the goodness of docking using a grid-based energy scoring function (Irwin and Shoichet, 2005). A defined docking protocol was employed to optimize the balance between the quality of the docking and the time required for the process.

Of the 72,766 compounds subjected to virtual screening with docking simulation, 3494 top-scored (dock score $\geq$50) compounds were selected. Six hundred sixty of them were selected for further evaluation based on consensus scoring (LigScore2, LUDI energy estimate 3, PLP 2, Jain, and PMF). Interestingly 99% of the compounds were found to have a carboxlyate group as a part of their structure. It is worth noting that most sialidase inhibitors known till recently, including natural products, contain a typical carboxylic acid group, and this reveals that the carboxylic acid group is an absolute necessity for sialidase inhibition. Next 37 compounds were selected based on the following criteria: (1) reasonable internal geometry of the ligand in the active site; (2) proximity of the carboxlyate group or relation to the arginine triad in the proposed binding mode; and (3) complementarity between the ligand and the protein surfaces, in terms of spatial occupancy and contacts in hydrophilic/hydrophobic regions. Of the 37 compounds selected, 13 of them (**5**–**17**) were selected based on their chemical classes and scores and were proposed as potential sialidase inhibitors (Table 1). The binding pose of hit compound **5** (Fig. 3) in NEU2 appears to have good steric and chemical complementarity with the active site. Moreover, the docked conformation was the best ranked in high-throughput docking and consensus scoring strategy. Specifically, its diacid moiety can form extra electrostatic interactions with the sialidase active site (interaction with the fourth arginine group Arg 41), and its flat furan ring with two aromatic side chains can make hydrophobic interactions with the active site (Fig. 3).

**Table 1** Structures of the hit compounds, with their consensus scores

| Compound | | Consensus scoring | | | | | |
|---|---|---|---|---|---|---|---|
| | | Dock | Ligscore | -PLP2 | -PMF | Jain | Ludi |
| **5** | 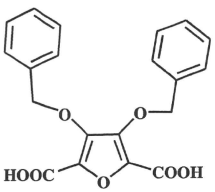 | **145.9** | **5.0** | **69.2** | **148.9** | **7.2** | **877** |
| **6** | 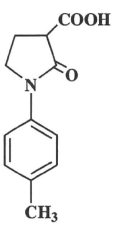 | 132.0 | 4.4 | 49.6 | 104.3 | 4.3 | 843 |
| **7** | 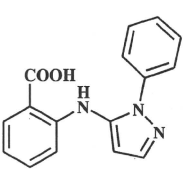 | 100.0 | 4.4 | 55.6 | 125.0 | 3.97 | 639 |
| **8** | 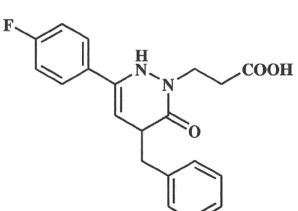 | 104.0 | 4.9 | 64.57 | 154.0 | 3.62 | 688 |

**Table 1** continued

| Compound | Consensus scoring | | | | | |
|---|---|---|---|---|---|---|
| | Dock | Ligscore | -PLP2 | -PMF | Jain | Ludi |
| **9** 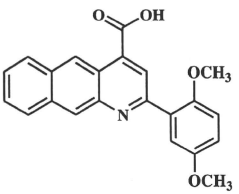 | 99.0 | 4.8 | 61.0 | 134.6 | 4.2 | 659 |
| **10** 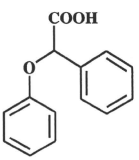 | 55.6 | 6.1 | 56.9 | 99.3 | 2.3 | 690 |
| **11** 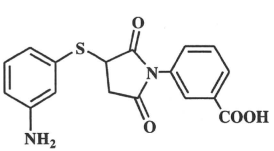 | 110 | 5.5 | 54.7 | 124.0 | 5.5 | 620 |
| **12** 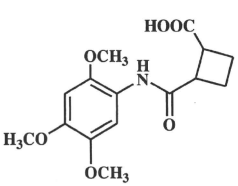 | 101.9 | 5.1 | 55.0 | 131 | 4.78 | 729 |

**Table 1** continued

| Compound | | Consensus scoring | | | | | |
|---|---|---|---|---|---|---|---|
| | | Dock | Ligscore | -PLP2 | -PMF | Jain | Ludi |
| **13** | 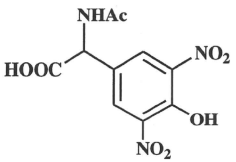 | 110.4 | 4.7 | 69.0 | 155 | 2.0 | 598 |
| **14** | 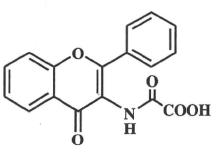 | 102.0 | 4.8 | 56.5 | 134.6 | 5.1 | 600 |
| **15** | 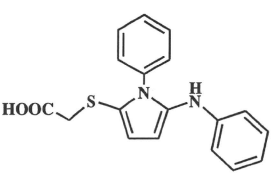 | 106.5 | 4.4 | 59.0 | 107.1 | 5.1 | 585 |
| **16** | 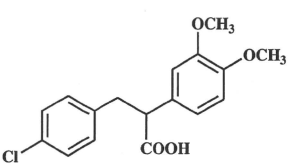 | 108 | 4.6 | 57.0 | 170.0 | 5.1 | 715 |

**Table 1** continued

| Compound | Consensus scoring | | | | | |
|---|---|---|---|---|---|---|
| | Dock | Ligscore | -PLP2 | -PMF | Jain | Ludi |
| **17** 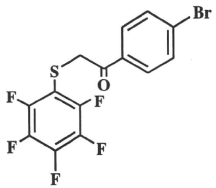 | 131.8 | 3.0 | 55.3 | 100.0 | 4.5 | 601 |

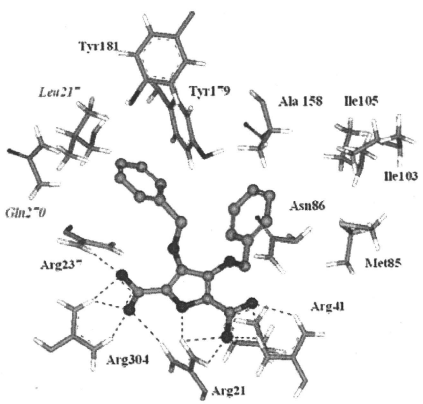


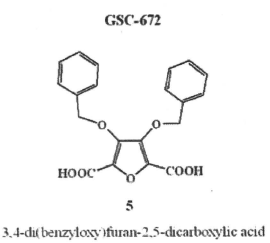


**Fig. 3** Proposed docking conformation of the hit (**5**) at the NEU2 active site. Only the parts of interacting residues are shown

Compound **5** (3,4-di(benzyloxy)furan-2,5-dicarboxylic acid) was purchased from Maybridge Chemical Co. and was screened against all human sialidases (NEU1–NEU4). The percentage inhibition (%I) against various concentrations ($\leq$1 mM) of compound **5** is shown in Fig. 4. Unexpectedly, compound **5** showed only moderate inhibition against NEU2 (%I = 40%), NEU3 (%I = 56%), and NEU4 (%I = 56%), whereas NEU1 (%I = 7%) was resistant to compound **5** activity at 1 mM. Calculated $IC_{50}$ values of NEU1, NEU2, NEU3, and NEU4 were >2 mM, >1 mM, 920 μM, and 670 μM, respectively (Table 2).

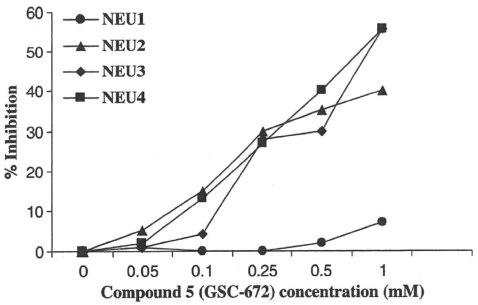


**Fig. 4** Inhibition of four types of human sialidases by compound **5**

**Table 2** Human sialidase (NEU1–NEU4) inhibitory activities of **5**, as well as some previously tested compounds

| Compound | Sialidase inhibition ($IC_{50}$ mM) | | | |
|---|---|---|---|---|
| | NEU1 | NEU2 | NEU3 | NEU4 |
| **2** (DANA) | 0.143 | 0.04 | 0.06 | 0.07 |
| **3** (GSC-649)[a] | 0.01 | >1 | >1 | >1 |
| **4** (GSC-697)[b] | –[c] | 0.55 | >5 | >5 |
| **5** (GSC-672) | –[d] | >1 | 0.92 | 0.67 |

[a] From Magesh et al. (2008)

[b] From Magesh et al. (2009)

[c] No inhibition at 1 mM

[d] Seven percent inhibition at 1 mM

To gain insight into the structural basis of the observed inhibition, we attempted to redock compound **5** into the crystal structure of NEU2 and other isoform models, which were predicted previously (Magesh *et al.*, 2006). Although not intentional, it is not surprising to see that the conserved Glu residue (in NEU2, Glu111, which was not included during the virtual screening run) that is present at the entrance of the active-site crevice can block the entry of the bulky phenyl group(s) of **5** into the active site (Fig. 5). As a result, compound **5** appears to have an irrational binding mode with the loss of few conserved interactions with the Arg triad in all isoform active sites. It is worth noting here that the Glu111 in the crystal structure of NEU2 stays far (16 Å) from the active site during open conformation, and upon binding of the substrate or inhibitor (DANA), it comes closer ($\sim$2.3 Å) and partially covers the active site (Chavas *et al.*, 2005). Thus, it appears that the weak activity of **5** compared to DANA-like compounds may be due to its inability to cope with the above-mentioned dynamic nature of the protein (induced fit behavior, reportedly specific to human sialidases) because of its steric tail ends. This also represents the potential of compound **5** as a novel frame structure for inhibitors of sialidases from